Microlensing Events with X-Ray Counterparts

Max Murphy
Astronomy 98
Harvard University, Cambridge, MA
December 11th, 2013

Advisor: Rosanne DiStefano
Group Members: Frank Primini, Ben Tunbridge, Idan Ginsberg

1. Abstract:

For the past two decades, microlensing has been a promising phenomenon for a variety of astronomy fields. Detecting small amplification of distant objects' flux has provided evidence of planetary star systems and faint, otherwise undetectable MACHOs, such as neutron stars and black holes. Identifying the locations of these previously unrecorded objects can provide more accurate details about the distribution of dark matter in the Milky Way's Galactic Bulge and dark Halo. Two broad scale sky surveys, The Optical Gravitational Lensing Experiment (OGLE) and Microlensing Observation in Astrophysics (MOA), record the luminosity of objects that appear to be involved in microlensing events and post a light curve of the desired event: the magnitude of the source object plotted vs. the approximate event duration in Julian days. Frank Primini, a coworker of Rosanne DiStefano and member a team of astronomers researching microlensing events, has developed a program to monitor the MOA and OGLE events and find possible catalogued object matches near the recorded position of each announced event. The events are matched with objects registered in a variety of catalogues, two of which include X-Ray source objects - the Chandra Source Catalogue (CSC) and the XMM-Newton Serendipitous Source Catalogue (3XMM-DR4). I present a general discussion and classification of the 38 matches between X-Ray objects and microlensing events recorded in the past decade, searching specifically for indications of Black Holes or Neutron Stars. I offer a visual representation of these events including the type of X-Ray radiation (soft--hard), separation between event and matched object, closeness of lens fit, literature references, and potential error in flux observations due to gas emitted from dust (Schlatly & Finkbeiner 1992). From the original 38 microlensing events, I noted eleven events having amplifications that poorly represent a microlensing light curve and nine events with limited observational data. The remaining eighteen events deserve

further observation and analysis before any other conclusions about their physical properties can be confirmed.

2. Introduction:

Almost 75 years before observing gravitational lensing events became a feasible technique, Einstein used his newly published theory of General relativity to correctly predict the amount of deflection that would occur when light from a distant object is distorted by the gravity of another object. However, he was unconvinced that this phenomena would occur frequently enough to contribute to observational astronomy (Einstein 1936).

Today, the study of gravitational lensing has evolved into a flourishing field of astronomy, contributing to the discovery of exoplanet systems and a better understanding of galactic mass distribution. Gravitational lensing events are divided according to the type of observed distortion into three main groups: strong lensing, weak lensing, and microlensing. Microlensing refers to a specific type of gravitational lensing where the multiple images and projections of Einstein rings normally seen in strong gravitational lensing phenomena cannot be distinguished.

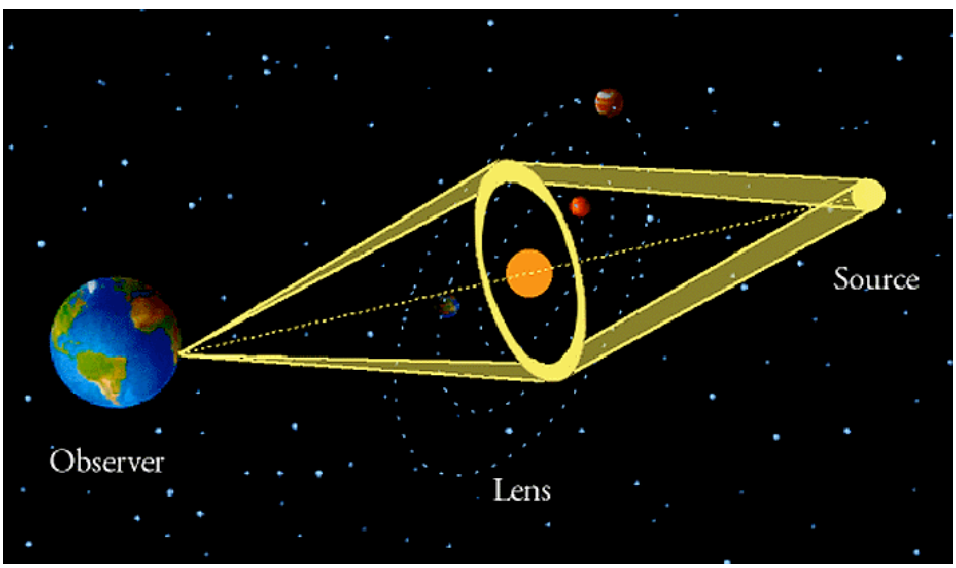

Image 1 - An illustration of gravitational lensing. A lens moves into the line-of-sight between an observer on Earth and a distant background source, amplifying the observed light.

http://www.universetoday.com/102466/early-galaxies-churned-out-stars-like-crazy/

The distortion from the lens' gravitational well appears as a "single object of increased apparent brightness" (Sutherland et al. 2001). As the lens crosses within the Einstein radius of the background source, the observed object appears to gradually brighten, peak, then symmetrically return to its normal luminosity. Wide-field surveys have found success in identifying microlensing events because of several unique signatures of the produced light curve: despite their surprising frequency, microlensing events are still rare enough that each object will only be lensed at most once every 50 years, allowing any quasi-periodic observations to be classified instead as a variable star. Secondly, a clean light curve of an event will be symmetrical about the peak and achromatic -- the deflection angle predicted by Einstein is not dependent on the wavelength of the source's light (Jovanic et al. 2008).

A paper written by Paczyński in 1986 suggested that microlensing, originally observed as effects from individual stars in a gravitational lensing event involving our galactic halo and another nearby galaxy, could be helpful for understanding the distribution of dark matter in the Milky Way -- namely that massive compact halo objects (MACHOs), such as neutron stars, black holes, and brown dwarfs, account for a majority of the mass in the galactic halo. These microlensing events were found to occur much more frequently than the originally predicted gravitational lensing phenomena, especially when observing through the Galactic Bulge and Halo towards high density regions such as the Magellanic Clouds, and became an increasingly popular topic for astronomy research. However, after sizable surveys by the astronomer groups MACHO and EROS using wide-field 1 m class telescopes, contradicting lensing records refuted the idea that MACHO's comprise most of the matter in the galactic halo, and cast doubt on the assumption that dark matter causes a majority of the microlensing events that we can observe in our galaxy. The MACHO team published their findings first, claiming that 20 per cent of the mass in the galactic halo are MACHO's with an average of 0.4 solar masses (Alcock et al. 2000). Seven years later EROS published their data, declaring that after over six years of observations no microlensing events indicated the presence of a MACHO, providing an upper limit to the galactic halo mass ratio of only 8 per cent (Tisserand et al. 2007).

Despite these setbacks, The Optical Gravitational Lensing Experiment (OGLE) at Las Campanas Observatory, Chile, continued the search for dark matter with microlensing phenomena in the Magellanic Clouds and Galactic Bulge, finding several hundred microlensing events each year. OGLE monitored the Large Magellanic Cloud during its second (1996-2000) and third (2001-2009) phases, OGLE-II and OGLE-III respectively (Wyrzykowski et al. 2012). The Microlensing Observations in Astrophysics (MOA) project, a joint operation initiated between Japanese and New Zealand astronomers in 2003 and based at the Mount John University Observatory near Lake Tepo, New Zealand, makes observations on dark matter as well as extra-solar planets and stellar atmospheres. The MOA team looks specifically for dark lenses in the galactic halo and bright sources in the Magellanic Clouds, placing particular emphasis on the determination of the distance to each lens. These surveys alert astronomers of new microlensing events multiple times each week during observing season (February - October), providing many new opportunities to find dark matter objects.

3. Classification:

We can assume that isolated neutron stars and black holes accreting interstellar medium should predominately emit X-Rays, but in order to filter for event matches that are MACHOs we must first consider the type of X-Ray emission that is being observed. X-ray radiation can be classified into two ranges: X-Rays with energies above 5-10 keV are considered "hard", while those with lower energy are designated as "soft". For a low accretion-rate neutron star, we can expect to see peak emission in soft X-Rays (Sartore et al. 2011). On the other hand, black hole behavior is quite different and not completely understood. Compared to neutron stars, black hole models indicate lower efficiency in converting accreted matter into X-Ray radiation, but with significantly higher mass the luminosities of black holes are approximately of the same order (Sartore et al. 2011). We cannot assume that black hole radiation will be dominant in the soft or hard range, because different regions emit varying energy levels. Typically, the accretion disk emits mainly soft X-Rays, while hard X-Rays are produced by a corona that surrounds the black hole.

We can compile data from both the Chandra Source Catalogue (CSC) and the XMM-Newton Serendipitous Source Catalogue (3XMM-DR4) for all objects that exist within two arcseconds of the microlensing event coordinates and emit X-Ray radiation. The CSC data is recorded in flux (normalizations of power-law and blackbody models that match the observed net X-ray counts provide the source energy flux data), and is divided into four bands -- broad (0.2-7.0 keV), soft (0.5-1.2 keV), medium (1.2-2.0 keV) and hard (2.0-7.0 keV). The Chandra team calculated hardness ratios between pairs of energy bands using the Bayesian algorithm (BEHR, Park et al. 2006) and sources with high signal to noise ratios are fitted using a modeling application called SHERPA (Freeman et al. 2001). The 3XMM-DR4 catalog divides their recorded flux into numerically ordered energy bands: (1) 0.2-0.5 keV, (2) 0.5-1.0 keV, (3) 1.0-2.0

keV, (4) 2.0-4.5 keV, and (5) 4.5-12.0 keV. 3XMM hardness ratios (HR), referred to as X-Ray "colors", are camera dependent and can be derived by combining corrected count rates from each energy band: $HR_n = (RATE_b - RATE_a) / (RATE_b + RATE_a)$, where HR_1 would combine energy bands 1 and 2.

The duration of a microlensing event is constrained by the time taken to cross twice the lens' Einstein radius, which is approximated to be $8(M_{lens}/M_{sol})^{1/2}$ AU (Sutherland et al. 2001). This angular width is considerably larger than the average size of MACHOs, so both lens and source objects can be can be assumed to be point sources. For a normal galactic speed of 200 km s^{-1}, the event duration is approximately 130 Julian days × $(M_{lens}/M_{star})^{1/2}$. If we assume a neutron star has a lower limit mass of 1.4 M_{sol}, then an event duration between 75-150 Julian days provides a good starting point for classifying light curves from MOA and OGLE databases as being associated with neutron star sized objects. In the case of a stellar black hole of 3 M_{sol}, the event duration would be between 150-250 Julian days. Both of these approximations for event duration assume that the involved black hole or neutron star is the lens and not the background source.

The presence of dust may also affect the probability that the luminosity magnification event observed is in fact a microlensing event. In areas of X-Ray radiation, such as an accreting neutron star, some dust rich in elements depleted from gas (Mg, Fe, Si, and Ca) will release these gases when bombarded by a supernova blast from a newly formed neutron star or black hole. Light from these X-Ray sources can increase sightly in luminosity as gas with the aforementioned elements have strong X-Ray lines. To account for possible dust interference, I used Schlafly and Finkbeiner's galactic extinction color correction data, recalibrated from the Schlegel, Finkbeiner & Davis 1998, Appendix B; 1998ApJ...500..525S (SFD98) infrared-based dust map. The corrected magnitude is recorded as A_λ and would be factored into a calculation of lens magnitude by: $M - m = 5(1 + \log(p)) + A_\lambda$, where M is the absolute magnitude, m is the apparent magnitude, and p is the parallax angle of source in arcseconds.

Finally, we can examine model fits of the light curves that OGLE and MOA produce for each event. These models, which typically consist of the symmetric rise and fall of peak amplification, provide a secondary check on microlensing luminosity constraints and eliminate luminosity amplifications due to phenomena not related to microlensing objects.

4. Event matches:

The following CSC X-Ray catalogue matches were made

Event	RA	DEC	Name	Sep	Max Sep
macho-105.21425.3499	18:06:08.513	-27:46:13.21	CXO J180609.1-274600	15.645	33.457
*moa-2003-BLG-30	18:05:07.11	-27:43:09.3	CXO J180507.0-274308	0.525	4.607
moa-2007-BLG-40	17:55:42.805	-28:18:09.18	CXO J175542.8-281809	0.779	5.109
ogle-2003-BLG-120	17:50:47.59	-29:30:05.0	CXO J175047.7-293012	7.393	8.605
ogle-2005-BLG-122	17:51:59.87	-29:31:49.0	CXO J175159.6-293146	4.185	4.737
ogle-2005-BLG-360	17:53:43.60	-29:41:52.8	CXO J175342.5-294151	13.347	21.530
ogle-2008-BLG-167	18:03:17.68	-29:51:10.4	CXO J180317.6-295110	0.580	5.053
moa-2010-BLG-097	17:53:31.73	-29:43:55.58	CXO J175331.4-294344	11.596	23.245
*ogle-2011-BLG-1540	17:54:55.68	-29:53:54.1	CXO J175455.6-295354	0.382	4.808
*moa-2012-BLG-295	17:51:13.61	-30:37:25.97	CXO J175113.6-303726	0.771	4.630
moa-2012-BLG-436	18:05:35.41	-29:57:49.74	CXO J180535.2-295750	2.451	11.697
ogle-2012-BLG-1133	17:51:26.53	-29:39:07.8	CXO J175126.5-293905	2.403	4.770
ogle-2013-BLG-0612	17:53:21.31	-28:32:00.0	CXO J175321.2-283159	0.745	4.759

The following 3XMM X-Ray catalog matches were made:

Event	RA	DEC	Name	Sep	Max Sep
macho-105.21425.3499	18:06:08.513	-27:46:13.21	3XMM J180608.5-274610	2.524	4.928
moa-2003-BLG-3	17:54:35.36	-27:44:59.8	3XMM J175435.3-274458	0.816	6.381
moa-2003-BLG-30	18:05:07.11	-27:43:09.3	3XMM J180507.0-274308		
moa-2003-BLG-72	18:05:22.55	-27:52:28.2	3XMM J180522.4-275231	3.316	7.203
moa-2004-BLG-3	18:05:40.51	-27:34:27.9	3XMM J180540.5-273428	1.100	5.320
moa-2007-BLG-171	18:05:26.481	-27:43:04.59	3XMM J180526.7-274302	4.552	6.550
moa-2007-BLG-331	18:17:56.789	-24:01:36.83	3XMM J181756.9-240137	2.995	5.440
moa-2007-BLG-411	18:08:52.242	-25:41:13.33	3XMM J180852.2-254113	0.504	5.592
moa-2008-BLG-180	17:54:51.025	-30:10:19.21	3XMM J175451.0-301019	0.926	8.854
ogle-2002-BLG-250	17:55:50.63	-29:50:10.9	3XMM J175549.9-295011	9.198	10.141
ogle-2004-BLG-419	18:06:49.21	-29:25:34.5	3XMM J180649.2-292531	2.892	6.292
ogle-2006-BLG-115	17:54:43.35	-30:01:19.2	3XMM J175443.2-300113	5.487	7.791
ogle-2007-BLG-247	18:09:14.79	-25:54:45.5	3XMM J180914.8-255446	1.542	6.611
other-ANG-08B-M31-06	0:42:39.3	+41:16:54.9	3XMM J004239.7+411655	4.900	6.523
other-L5	00:42:59.5	+41:14:17	3XMM J004300.2+411437	22.288	32.312
moa-2010-BLG-067	18:05:08.97	-27:41:49.66	3XMM J180508.7-274150	3.220	5.886
moa-2010-BLG-168	18:09:14.70	-25:52:05.74	3XMM J180914.6-255204	1.560	6.600
ogle-2011-BLG-1540	17:54:55.68	-29:53:54.1	3XMM J175455.6-295353	0.887	5.336
moa-2012-BLG-295	17:51:13.61	-30:37:25.97	3XMM J175113.7-303723	3.258	4.901
ogle-2012-BLG-0391	17:56:03.21	-28:52:38.8	3XMM J175603.1-285234	4.749	6.086
ogle-2012-BLG-0971	17:55:13.91	-29:39:56.3	3XMM J175513.9-293946	9.636	44.340
ogle-2012-BLG-1422	17:50:54.43	-29:49:32.8	3XMM J175054.6-294936	4.796	7.902
ogle-2012-BLG-1698	17:53:39.13	-29:49:00.8	3XMM J175338.7-294915	16.161	19.354
moa-2013-BLG-128	17:55:16.355	-29:36:52.760	3XMM J175516.5-293653	2.464	4.848
moa-2013-BLG-147	18:02:22.050	-32:52:57.146	3XMM J180222.0-325254	2.496	6.255
ogle-2013-BLG-0769	18:05:05.39	-27:49:21.7	3XMM J180505.1-274922	2.739	5.368

Table 1 is a record of all microlensing events in the past ten years that occurred near a catalogued X-Ray source. Their position is recorded as Right Ascension (RA) and Declination (DEC); the name of the catalogued object and it’s separation from the event is included (with error). The “*” in the first group denotes events that had matches in both catalogues.

5. Catalogue Matches:

Using the right ascension (RA) and declination (DEC) position coordinates of each microlensing event with an object match in the CSC catalog, I used the interactive software Sky Atlas Aladin (http://aladin.u-strasbg.fr) to access the Chandra Source Catalogue data (CSC_full, downloaded from their website). Aladin processes the catalogue data, presenting an interactive map, which I used to examine the location of each microlensing event and record the closest X-Ray source. I made note of any event did not have a clear match (i.e. multiple sources exist within two arcseconds of the event). Image 2 shows a number of CSC objects as red triangles in the Aladin display. For each object in the catalog, CSC provides position and flux data, as specified in section 3, which can be accessed by highlighting an object in Aladin. For each object, I recorded the CSC flux bands soft through broad, their positions in galactic latitude and longitude, and the separation in arcseconds between the CSC object and the OGLE or MOA coordinates. Error in the position coordinates of the catalogued object range from 0.5-3.0”. It is also worth mentioning that there are some discrepancies between the recorded positions of OGLE and MOA events, on average about 0.05”. In addition, MOA and OGLE occasionally record the same event, but small differences in the recorded position result in the observations appearing to be separate events. These errors are most likely due to the algorithm used to compute each location based on the telescope position.

Image 2

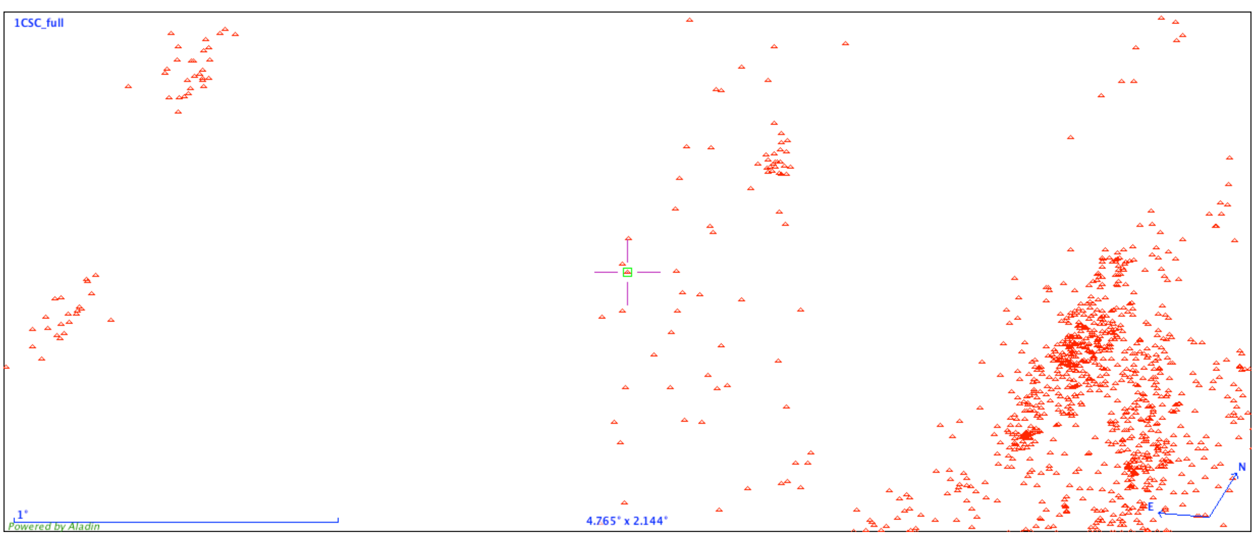

I replicated the same procedure for the events matched with 3XMM objects, but instead using the 3XMM_DR4cat file from the 3XMM webpage as a sky map in Aladin. Again I recorded their standard flux in the five X-Ray energy bands specified for this catalogue in section 3, as well as the object position coordinates and separation from the matched event (in arcseconds). I also accessed the online NASA/IPAC Extragalactic Database (NED), which includes data from Schlafly and Finkbeiner's infrared-based dust map. By searching for each object via their RA and DEC, I recorded an associated color correction magnitude (A_λ) due to the existance of dust in the field of view. While this magnitude is not explicit evidence for the presence of X-Ray radiating gasses, highly concentrated areas of dust will be affected by the presence of a nearby accreting black hole or neutron star participating in a lensing event. In order to detail the potential significance of each event, I plotted 20 events whose light curves closely resemble microlensing curve fits according to their longitude and latitude. I layered events affiliated with multiple categories with colored circles, each representing a different reason why that event is worth analyzing.

Image 3

In image 3, the triangle points represent the position of each object found in the CSC and 3XMM catalogs whose microlensing event accurately matches light curve models used by the OGLE and MOA without significant error from limited observation. The *red* rings indicate objects with predominately soft X-Ray emission, as calculated by OGLE and MOA flux ratio techniques detailed in section 3, and indicate possible evidence for a neutron star lens.The *green* rings identify objects with low angular separation between the event and the known location of the associated X-Ray source. The *orange* rings signal low magnitude correction due to the presence of gas from dust, and the *blue* rings indicate objects referenced in literature that is available on the SAO/NASA Astrophysics Database System (ADS).

6. Light Curves:

In the following section, I will examine a selection the matched objects that appear to be good candidates for MACHOS. This is not an exhaustive list of all X-Ray matches that involve neutron stars or black holes, because some of the events may not be clean observations and others won't exhibit all of the usual indicators of MACHOs.

Image 4 - The light curve of the 2013 OGLE event BLG-0769. The y-axis is presented in magnitude in the I band magnitude (0.79 μm), and the x-axis is given in Julian days.

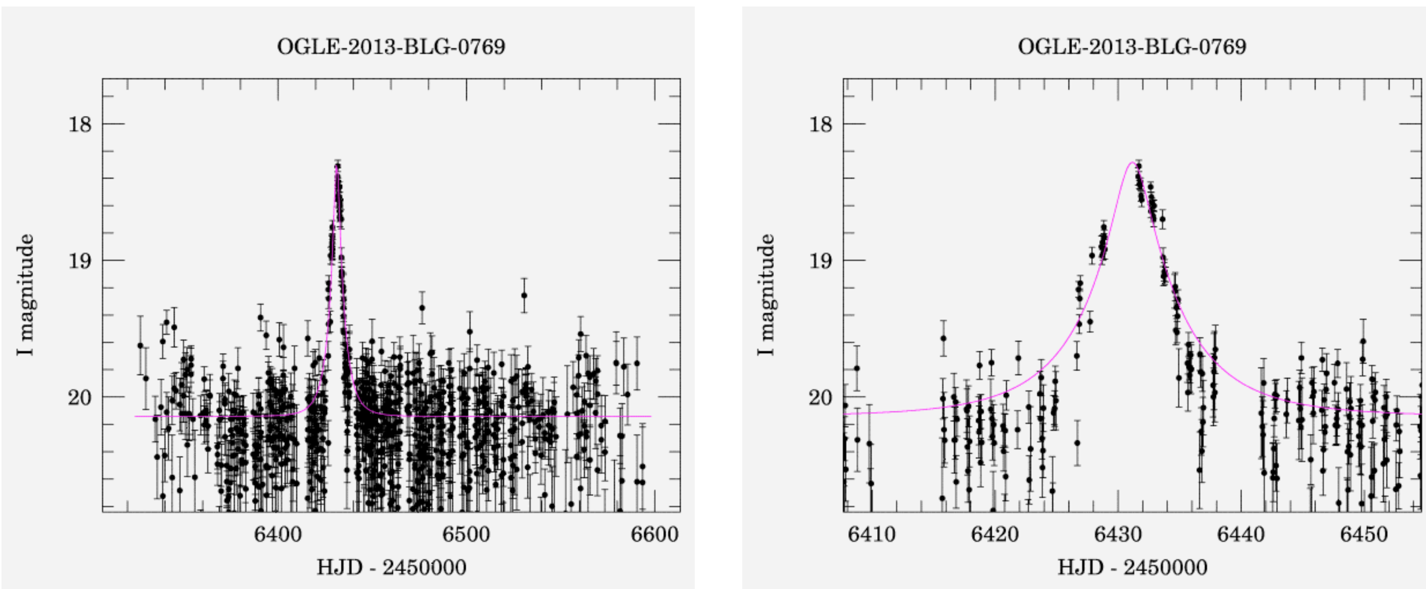

In image 4, the left graph is a representation of observed flux over the past recording season, showing a significant amplification with a duration of 25 Julian days. The amplification factor from OGLE data is 5.546, showing a substantial increase of the object's initially faint luminosity (20.2 mag), and the microlensing curve fit appears to match the data well. There is no evidence of a folded curve (either rising or dropping much faster than predicted) and the amplification was recorded without major breaks in observation, indicated by the quantity of data around the event. One constraint on the probability that this event involved a MACHO object is the short event duration, only 25 days. Object data recorded from the 3XMM catalogue indicates that this X-Ray emission as mostly in the hard (2 - 7 keV) spectrum. This would most-likely eliminate an accreting neutron star as a lens object. Although black holes also emit hard X-Rays, we cannot accurately classify this as a quasar or wandering black hole without further analysis of the object’s spectral and physical properties.

Image 5 - The light curve of the 2010 MOA event BLG-097. The y-axis is presented in delta flux (× 10^{-15}), and the x-axis is given in Julian days.

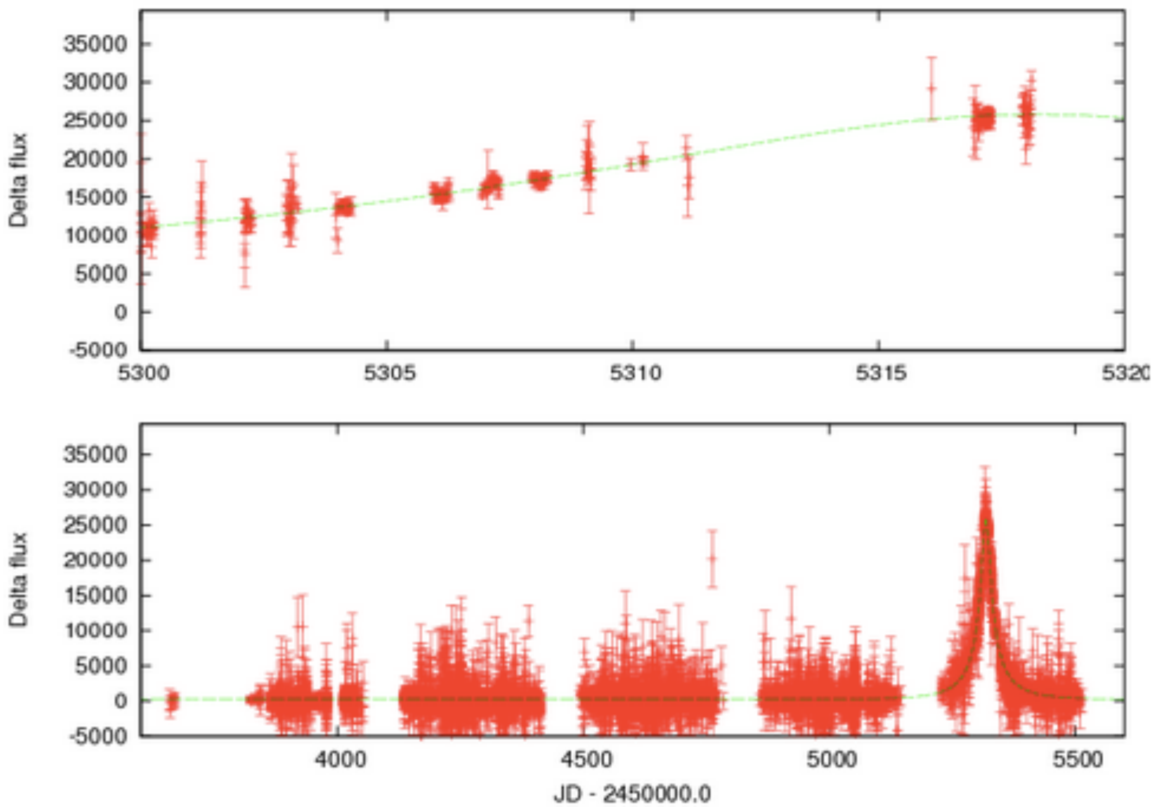

The MOA light curves in image 5 appear slightly different than the OGLE data, but in fact convey similar information. The top graph indicates an amplification of about 2.45 on the baseline I magnitude of 18.88 mag. This event has a long event duration of 90.84 Julian days, and the top graph is not formatted to correctly portray they length of the microlensing event. Despite the poorly chosen graph parameters, the observation appears to have fully recorded the event, and the flux data accurately replicates the calculated lens fit, showing no signs of a folded curve. Soft X-Rays between 0.2 and 1 keV dominate BLG-097's emission spectra, possibly indicating the presence of an accreting neutron star. The 3XMM catalog object matched to this event also has a low color correction magnitude, allowing more trust in the accuracy of X-Ray flux measurements.

One particularly interesting event, recorded as both 2004-BLG-04 in MOA and 2004-BLG-081 in OGLE, was referenced in Sartore and Treves' Matching Microlensing Events with X-Ray sources (http://arxiv.org/abs/1112.4203). The MOA data is untrustworthy because a close examination of the recorded event duration and the duration of the luminosity amplification shows a noticeable difference in value. However, the OGLE data is recorded without large error and can be used to classify the object.

Image 5 - The light curve of OGLE event BLG-081 recorded in 2004. The y-axis is measured in I mag, and the x-axis Julian days.

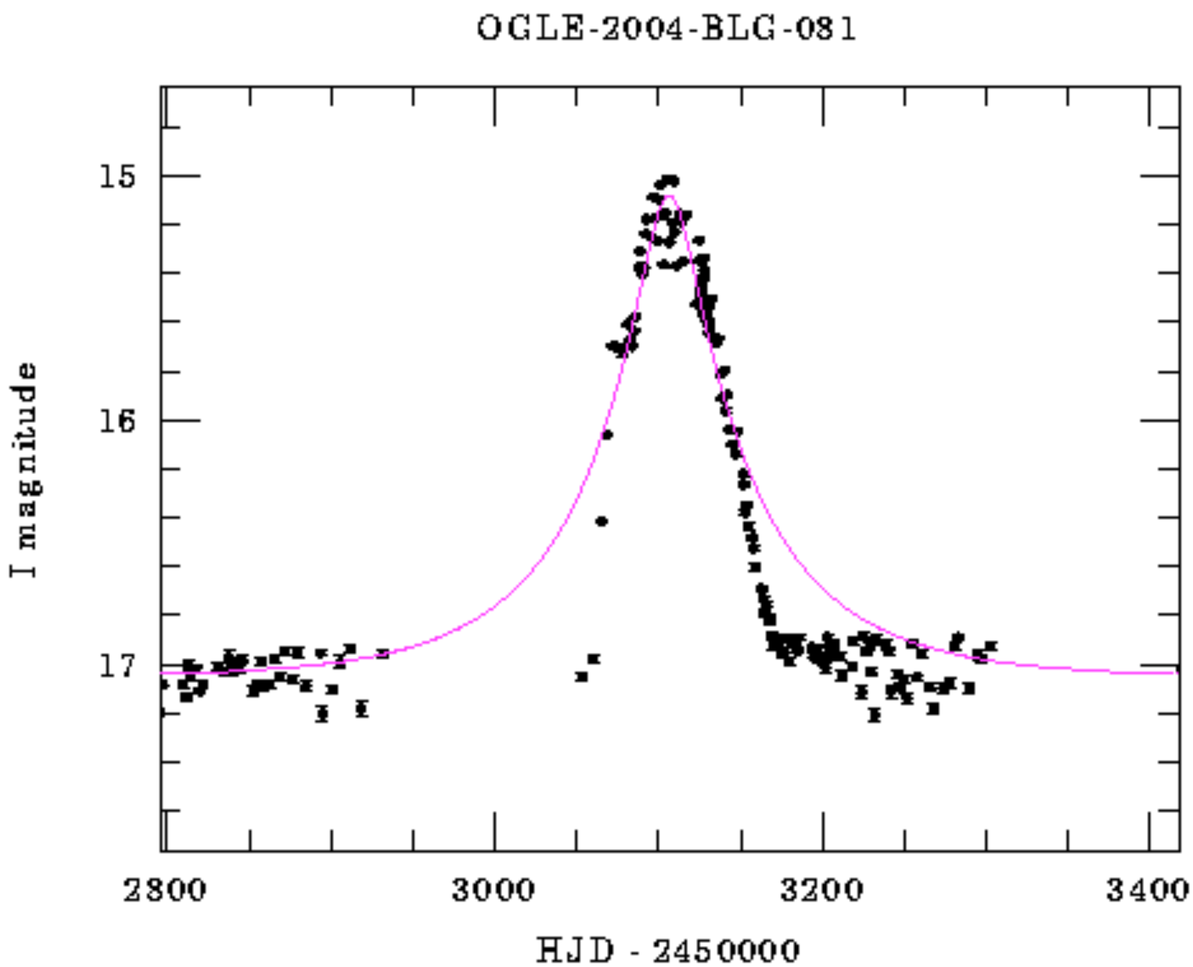

From OGLE data, we know that the Period is 103.63 Julian days and the baseline magnitude of the object before amplification is 17.06 mag, with a maximum amplification to 15 mag. The X-Ray spectra shows a distinct lack of soft X-Rays, indicating that the object is probably not a neutron star, but still possibly a black hole (Sartore and Treves). However, an unusually quick rate of amplification results in a poor fit for a microlensing event light curve. We can conclude that this event was not caused by microlensing, but perhaps some other form of luminosity amplification. In 2006, Wyrzkowski wrote a paper detailing this objects periodic nature outside of the OGLE and MOA observations - amplifications every four days. The paper suggested that the observed amplification could be an eclipsing binary source, or possibly an outburst from an accreting white dwarf, but not a genuine microlensing event. This event is therefore not included in the plotted list of high potential events.

7. Conclusion & Discussion:

From the original 38 events, six were both accurate fits to OGLE and MOA microlensing light curve models and possessed spectral properties neutron stars: moa-2012-BLG-436, ogle-2011-BLG-1540, ogle-2008-BLG-167, ogle-2004-BLG-419, moa-2012-BLG-295, and ogle-2012-BLG-1698. Of the remaining 23 events with good microlensing curve fits, ten had stronger emissions in the hard X-Ray band, indicating radiation from a wider range of star types and possibly black holes. I did not successfully detect the presence of a neutron star or black hole without significant doubt, but further analysis of these promising events, taking into account more accurate constraints, may yield more answers. More detailed observations of the source and lens objects in these events could provide better constraints on the type of object involved. For example, considering longer periods of observation to identify repeating or periodic events can provide evidence for variable stars. Also, further attempts to classify neutron star and black hole events will create a better understanding of the spectral properties of MACHO microlensing. A future step would be to develop an accurate lens fit model for specific types of microlensing events, such as those involving a neutron star in the Halo and a distant background object. Coupled with the increasingly precise models for black hole and neutron star evolution, microlensing will continue to provide enlightening information regarding the distribution of dark matter in the galactic halo.

During the observing season, new microlensing events are recorded by the OGLE and MOA teams every couple of days, providing many more opportunities for successful classification of the lens and source obejcts. X-Ray object surveys like the Chandra Source Catalog and 3XMM also update their databases annually with newly discovered X-Ray radiating objects and more accurately observed data. As we continue to build a complete historical database of all X-Ray microlensing events and our understanding of the complex properties of involved objects improves, detecting MACHO objects in the galaxy will become an achievable goal. Applying widely available analytical techniques to objects involved in gravitational microlensing will contribute dramatically to models of dark matter distribution and our understanding of how intergalactic objects interact.

Works Cited

Alcock C 2000 *The Astrophysical Journal* **452** 1

Jovanic P 2008 *Monthly Notices of the Royal Astronomical Society* **386:** 397-406

Paczynski B 1996 *Ann. Rev. Astron. Astrophys.* **34** 419

Sakano M 2002 *The Astrophysical Journal Supplement Series* **138**:19-34

Shlaftly E & Finkbeiner D *Recalibrated Infrared-based Dust Map* http://adsabs.harvard.edu/cgi-bin/nph-bib_query?bibcode=2011ApJ...737..103S&db_key=AST&high=3290e5e17909355

Sutherland W 2001 *Encyclopedia of Astronomy and Astrophysics* Nature Publishing Group

Wyrzykowski L 2012 *Acta Astronomica* **60** 17